Journal of Green Chemical and Environmental Engineering
e-ISSN: 3090-2568 | p-ISSN: 3109-2233
Journal Homepage: www.ejournal.candela.id/index.php/jgcee
Vol. 2, No. 2, July 2026

Article

Analysis of the Role of Iron (Fe) Content on Nickel Distribution in Limonite and Saprolite Zones Using Energy Dispersive X-Ray Fluorescence (ED-XRF)

James William Ariend*, Ismail Marzuki

Department of Chemical Engineering, Faculty of Engineering, Universitas Fajar, Makassar, Indonesia

ARTICLE INFO

Received: *30 April 2026*
Revised: *8 July 2026*
Accepted: *10 July 2026*

Keywords:
Lateritic nickel;
ED-XRF analysis;
Limonite zone;
Saprolite zone;
Geochemical distribution.

Corresponding author:
jameswilliamariend@gmail.com

DOI: *10.63288/jgcee.v2i2.26*

ABSTRACT

Nickel (Ni) is a strategic metal widely used in stainless steel, rechargeable batteries, aerospace, and renewable energy technologies. Increasing demand for electric vehicle batteries has intensified exploration of lateritic nickel deposits, which consist of limonite and saprolite horizons with distinct geochemical characteristics. This study investigates the relationship between iron (Fe) and nickel distribution in lateritic profiles using Energy Dispersive X-Ray Fluorescence (ED-XRF). Samples were collected from PT. Genba Multi Mineral, North Morowali, Indonesia, at depths of 1-6 m. Limonite samples were obtained from 1-3 m, while saprolite samples were collected from 4-6 m. After drying, crushing, and sieving to 200 mesh, the samples were analyzed by ED-XRF. The results reveal an inverse relationship between Fe and Ni contents. The limonite zone contained high Fe (48.76-50.23%) but relatively low Ni (0.70-1.15%), whereas the saprolite zone showed lower Fe (21.01-29.41%) and higher Ni (1.45-2.05%). These trends agree with lateritic nickel enrichment processes, in which Fe is concentrated in limonite while Ni becomes enriched in silicate-rich saprolite during weathering. The findings indicate that Fe content is a useful indicator of nickel distribution in lateritic deposits. In addition, ED-XRF proved to be a rapid, non-destructive, and reliable technique for multi-element analysis of laterite samples. This study provides geochemical information that can support nickel exploration, resource evaluation, and mining optimization in lateritic environments.

1. Introduction

Nickel has emerged as a critical raw material for modern industrial development, serving essential roles in stainless steel manufacturing, aerospace applications, electrochemical industries, and renewable energy technologies [1]. The rapid expansion of electric vehicles and lithium-ion battery production has significantly increased global nickel demand, drawing greater attention to economically viable nickel resources [2], [3]. Among these, lateritic nickel deposits account for a large share of global reserves and are widely explored due to their substantial resource potential [1], [4]. Formed through intense tropical weathering, laterite profiles consist of distinct limonite and saprolite zones that require different processing approaches, including High-Pressure Acid Leaching (HPAL) and Rotary Kiln Electric Furnace (RKEF) technologies [5], [6]. As one of the world's leading nickel-producing countries, Indonesia plays a pivotal role in the global supply chain, highlighting the importance of integrating geological exploration, resource estimation, and environmental assessment to ensure a sustainable and low-carbon nickel supply for future energy and infrastructure needs [7], [8].

Indonesia’s prominence as a global nickel producer stems from extensive tropical ultramafic-hosted laterites, notably in Sulawesi and Maluku, formed by prolonged weathering of serpentinized peridotites and related ultramafic rocks under humid tropical climates [5], [6], [9]. The classic laterite profile consists of a saprolite horizon rich in Mg-silicates (serpentine, garnierite, talc-related phases) beneath an oxide-dominated limonite zone enriched in Fe oxy-hydroxides (goethite, hematite) near the surface,

with systematic downstream enrichment of Ni in the saprolite and potential remobilization during goethite aging [2], [9], [10]. In Indonesian deposits such as Morowali (Sulawesi), Soroako/Pomalaa areas, and other ophiolite-derived profiles, Ni occurs primarily in garnierite- and serpentine-type Mg-silicates in saprolite, whereas limonite hosts Ni-bearing Mn-oxyhydroxides and goethite-related phases; nickel distribution is tightly linked to Fe-Ni interactions and redox/solid-state transformations within each horizon [4], [11]. This integration of mineralogy and geochemistry informs exploration targeting, ore delineation, and sustainable mining in a rapidly expanding global Ni market dominated by stainless steel and battery materials [9], [12].

Nickel currently forms a cornerstone of global laterite deposits, which are classic products of prolonged tropical-weathering of ultramafic parent rocks, this weathering drives a vertical zonation that typically comprises an upper limonite horizon and a deeper saprolite (silicate-hosted) horizon, separated by a transitional zone, with goethite/hematite prevailing in the limonite and serpentine, olivine-bearing phyllosilicates and other Mg-silicates concentrating Ni in the saprolite, a pattern repeatedly documented in Sta. Cruz-type profiles, and across Southeast Asia, New Caledonia, and other tropical [13], [14], [15]. The leaching enrichment dynamics during intense weathering preferentially remove mobile elements such as Mg, Ca, and Si from upper horizons, while relatively immobile elements including Fe accumulate near the surface, establishing the characteristic Fe-rich ferruginous cap; this Fe-Ni interaction is central to controlling Ni distribution, as high Fe contents in the limonite restrict Ni mobility and subsequent Ni enrichment, whereas Fe depletion deeper in saprolite facilitates Ni migration and accumulation in Ni-host minerals such as serpentine-type Mg-silicates and garnierite in the saprolite, with Ni concentrations commonly highest in the saprolite zone and occasionally redistributed into lateritic garnierite veins in transitional or deeper subzones [16], [17]. The limonite zone therefore typically exhibits high Fe but modest Ni enrichment due to strong Ni adsorption by iron oxyhydroxides, while the saprolite zone-rich in Mg-silicates like serpentine and lizardite–hosts the principal Ni stock, including Ni-bearing phyllosilicates and garnierites formed via Mg^{2+}-Ni^{2+} exchange during serpentinization and subsequent weathering; this understanding is reinforced by mineralogical and geochemical characterizations of Ni-laterite profiles that show systematic Ni mobility scaling with UMIA, pH, Eh, and the evolving Fe-Ni mineral equilibria across horizons [18]. The general model posits that Ni enrichment correlates with deepening weathering intensity and transition zone activity, where Fe is progressively depleted from limonite to saprolite, Ni-bearing silicates become established in the saprolite and transitional zones, and goethite crystallinity and Ni incorporation within goethite evolve with depth and Ni exposure, implying possible remobilization of Ni into garnierite veins as aging goethite ages through the profile [19]. Collectively, these studies converge on a framework in which the Fe–Ni interplay, modulated by climate-driven weathering, mineral transformation, pH and Eh conditions, and the evolving mineralogy of serpentinized ultramafics.

Previous studies have investigated lateritic nickel deposits using analytical techniques such as X-Ray Fluorescence (XRF) [3]. Most studies reported that limonite zones are enriched with Fe, while saprolite zones contain higher nickel concentrations. However, many previous investigations focused mainly on qualitative elemental characterization and did not quantitatively evaluate the direct relationship between Fe and Ni distribution using Energy Dispersive X-Ray Fluorescence (ED-XRF) as a rapid and non-destructive analytical method. In addition, studies concerning depth-dependent Fe–Ni distribution in lateritic deposits from North Morowali [6], Indonesia, remain limited. This condition indicates the existence of a research gap regarding quantitative geochemical relationships between Fe and Ni within Indonesian lateritic profiles.

Therefore, this study aims to evaluate the influence of Fe content on nickel distribution within limonite and saprolite zones using ED-XRF analysis. The study also seeks to identify depth-dependent

geochemical patterns and explain the mechanisms responsible for nickel enrichment within lateritic weathering systems.

2. Research and Methodology

2.1 Research Design

This study employed a quantitative field-based geochemical approach to investigate the vertical distribution and relationship of iron (Fe) and nickel (Ni) in lateritic nickel deposits. The research integrated field sampling, laboratory preparation, ED-XRF elemental analysis, and statistical evaluation to characterize geochemical variations within laterite profiles.

The study focused on two principal weathering zones, namely limonite and saprolite, which represent contrasting stages of lateritic evolution. The limonite zone is dominated by Fe-oxyhydroxides, while the saprolite zone is enriched in Mg-silicate minerals hosting nickel. Depth was used as a proxy for weathering intensity to evaluate vertical geochemical trends and element mobility within the profile.

Systematic sampling was conducted at different depths to assess Fe and Ni distribution along the lateritic sequence. Samples were air-dried, crushed, and sieved to 200 mesh prior to analysis to ensure homogeneity. Elemental concentrations were determined using calibrated ED-XRF, providing rapid and non-destructive multi-element quantification.

The workflow comprised field sampling (figure 1), sample preparation, ED-XRF analysis, and data processing, including graphical and statistical evaluation of Fe-Ni relationships. This design enabled assessment of vertical geochemical variation associated with lateritic weathering processes and provided a robust framework for interpreting Fe-Ni distribution patterns across limonite and saprolite horizons.

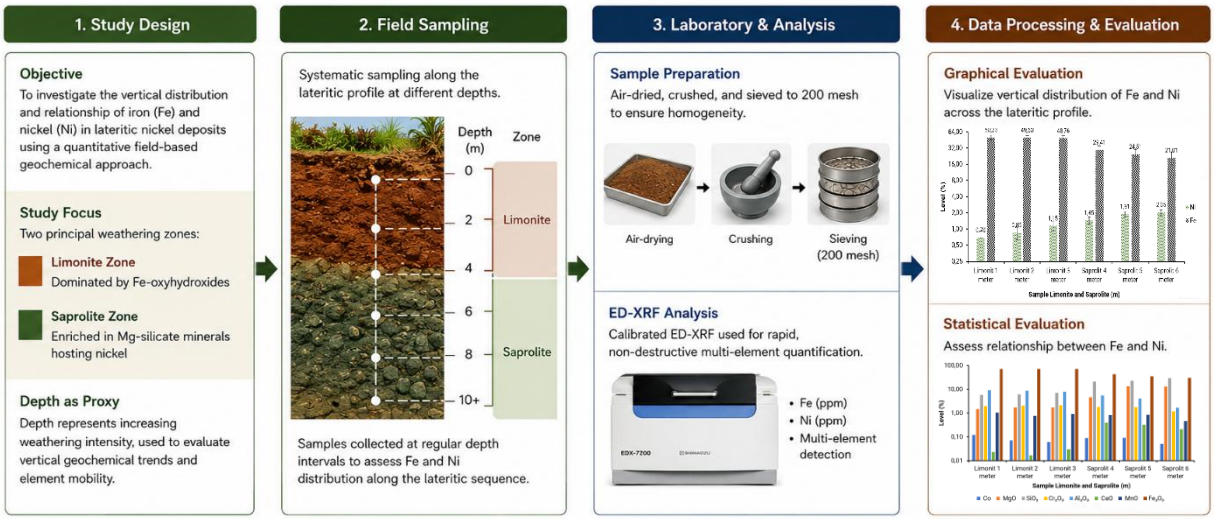

Figure 1. Schematic workflow of the research methodology

2.3. Materials and Equipment

The materials used in this study consisted of lateritic nickel samples collected from limonite and saprolite zones at depths of 1-6 m. All samples were air-dried, crushed, and sieved to 200 mesh prior to analysis to ensure homogeneity.

The equipment used included field sampling tools (hand auger and collection tools), laboratory sample preparation equipment (drying trays, crushers, and sieves), and analytical instrumentation in the form of an ED-XRF spectrometer for elemental determination. The ED-XRF system was used to quantify iron (Fe) and nickel (Ni) concentrations in weight percent (% wt) under calibrated measurement

conditions using certified reference materials. All samples were stored in sealed containers prior to analysis to prevent contamination and ensure sample integrity.

2.4. Sampling Procedure

In the sampling stage, nickel laterite materials were collected from field-identified limonite and saprolite zones based on visible weathering characteristics and profile observation. Within each zone, three representative samples (~100 g each) were collected at depths of 1-3 m (limonite) and 4-6 m (saprolite) to capture vertical variations in Fe and Ni distribution. Sampling was conducted using a systematic depth-based approach to represent geochemical changes across the lateritic profile. Each sample was immediately placed in a clean, sealed, and labeled container to prevent contamination and ensure traceability according to depth and zone classification.

2.5. Sample Preparation

The sample preparation stage began with a drying process using an oven at 105°C until the sample weight reached a constant state. This process aimed to remove the moisture content in the samples to ensure more accurate elemental analysis results. After drying, the samples were crushed using a crusher into a fine powder. The resulting powder was then filtered using a 200-mesh sieve to ensure a uniform particle size that meets analysis standards. Subsequently, 5 grams of the sample powder were weighed using an analytical balance with a precision of 0.0001 grams. This step was performed to ensure that the amount of sample analyzed met the requirements of the Energy Dispersive X-Ray Fluorescence (EDXRF) instrument.

2.6. ED-XRF Analysis Procedure

Elemental analysis was conducted using Energy Dispersive X-Ray Fluorescence (ED-XRF), a rapid and non-destructive technique for multi-element characterization of lateritic nickel samples. The instrument was calibrated using certified standard reference materials to ensure analytical accuracy and reproducibility.

Crushed and homogenized samples (200-mesh) were placed in sample holders and analyzed under standardized measurement conditions. Each sample was measured in triplicate, and the average values were used for subsequent geochemical and statistical analyses. The ED-XRF system quantified elemental concentrations as weight percentages (%wt), with a focus on Fe and Ni distributions across the lateritic profiles.

2.7. Iron (Fe) Content Analysis Using Energy Dispersive X-Ray Fluorescence (EDXRF)

In the iron (Fe) content analysis stage, the ED-XRF instrument was first calibrated to ensure the accuracy and reliability of the measurement results. The prepared sample powder was placed into a specialized container designed for X-ray analysis. The container holding the sample was then placed in the analysis chamber of the ED-XRF instrument, and the scanning process was executed using predetermined parameters. When X-rays are directed at the sample, electrons in the inner shells of the atoms are displaced, producing fluorescence X-rays with characteristic energies for each element. The instrument automatically detects the energy of these fluorescence rays and displays the iron (Fe) content measurement in weight percent (%wt). To ensure the accuracy of the results, replication and data verification were conducted by analyzing each sample three times (in triplicate).

3. Results and Discussion

3.1. Depth-Dependent Distribution of Fe and Ni

The variation of Fe and Ni concentrations based on depth is presented in Figure 2. The obtained results clearly demonstrate systematic geochemical differentiation between limonite and saprolite zones within the lateritic profile.

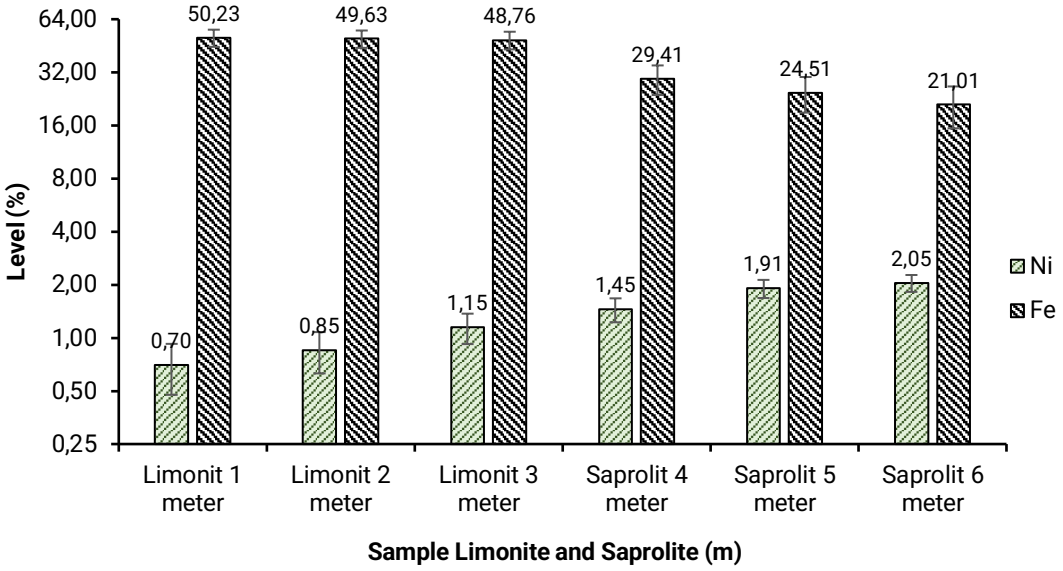

Figure 2. The analysis results of the effect of Fe on Ni show a significant increase in hardness.

Analyses indicate a clear vertical geochemical gradient with an inverse Fe-Ni relationship along the lateritic profile. The limonite zone (1- 3 m) is Fe-dominated, with Fe reaching ~50.23% at 1 m and slightly decreasing to 48.76% at 3 m, while Ni remains low (0.70-1.15%) [20]. These Ni levels are below typical high-grade saprolite economic thresholds for pyrometallurgical processing but remain relevant for hydrometallurgical recovery routes. The observed limonite composition suggests potential suitability for atmospheric acid leaching (HCl or H_2SO_4 - based systems) and other low-temperature hydrometallurgical processes, where Ni can be selectively extracted despite high Fe content. Previous studies show that Ni recovery from limonite is strongly controlled by leaching conditions such as pH, acid type, and temperature, which influence Ni selectivity over Fe. As reported in Ni–Co laterite processing literature, limonite ores are generally more amenable to hydrometallurgical routes such as HPAL or atmospheric leaching compared to saprolite, particularly for low-grade ores where pyrometallurgical processing is less economical [21], [22]. Process optimization strategies, including controlled leaching conditions and downstream Fe removal, are essential to improve Ni recovery efficiency in limonitic ores.

The analytical results reveal a systematic vertical chemical gradient characterized by a distinct inverse relationship between Fe and Ni concentrations across the lateritic profile. In the limonite zone (1-3 m), the geochemical environment is strongly Fe-dominated, with Fe concentrations peaking at 50.23% at 1 m depth and gradually decreasing to 48.76% at 3 m, while Ni remains relatively low, ranging from 0.70% to 1.15%, values that are generally below the economic cut-off grade for high-grade saprolite ore smelting but remain relevant for hydrometallurgical processing. A marked geochemical transition is observed at the limonite–saprolite boundary (between 3 and 4 m), where Fe concentrations decrease sharply from 29.41% at 4 m to 21.01% at 6 m in the saprolite zone, coinciding with a significant enrichment of Ni from 1.45% to a peak of 2.05% at 6 m [19], [21]. This strong vertical differentiation

and inverse Fe-Ni trend are consistent with established lateritic weathering models under tropical conditions [2], [8], where hypergene alteration promotes the immobilization and precipitation of Fe as secondary oxides and oxyhydroxides in the upper profile, while Ni exhibits relatively higher mobility, facilitating downward migration via percolating groundwater and subsequent accumulation in deeper saprolite horizons under contrasting physicochemical conditions [1], [3], [22].

3.2. Analysis Results of Other Components

Testing conducted using Energy Dispersive X-Ray Fluorescence (EDXRF) did not only detect the Fe and Ni content in the samples but also identified other elements contained within. The results of the analysis for other components are as follows:

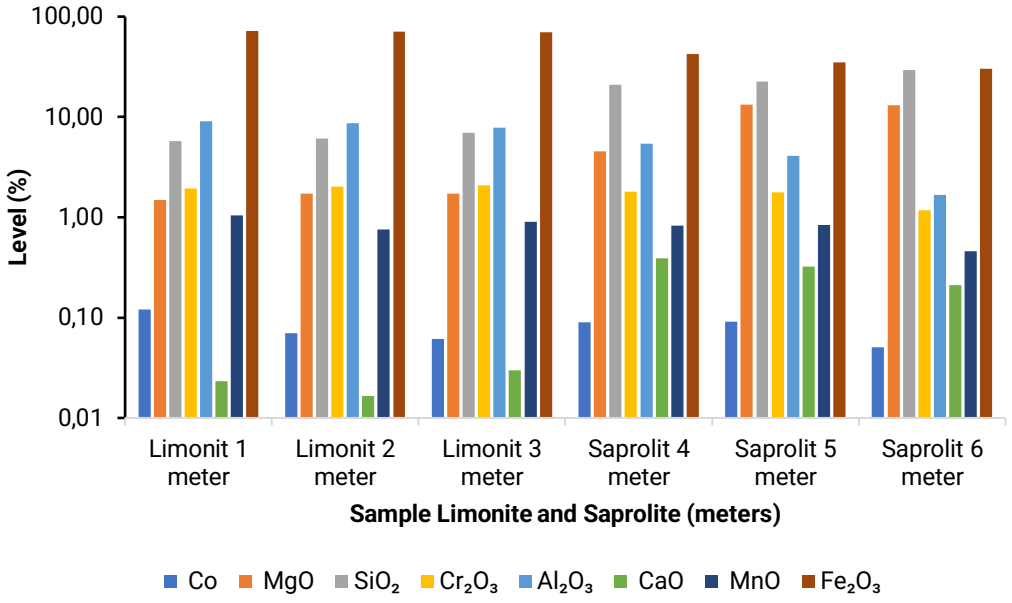

Figure 3. Results of Other Components Analysis

Based on the data presented in Figure 3, the nickel (Ni) grade shows a clear depth-dependent enrichment pattern across the lateritic profile, increasing progressively from the limonite to the saprolite zone. In the limonite zone (1-3 m), Ni concentrations gradually rise with depth, from 0.70% at 1 m to 0.85% at 2 m and reaching 1.15% at 3 m. A more pronounced increase is observed in the saprolite zone (4–6 m), where Ni grades continue to increase from 1.45% at 4 m to 1.91% at 5 m, reaching a maximum of 2.05% at 6 m. This systematic enrichment trend reflects the typical geochemical behavior of lateritic nickel systems, where nickel is progressively redistributed and concentrated in deeper saprolitic horizons during prolonged tropical weathering of ultramafic rocks. Recent studies on laterite geochemistry and nickel ore formation consistently report that saprolite zones act as the principal reservoir for Ni enrichment due to silicate-hosted incorporation and secondary mineral formation under evolving pH-Eh and leaching conditions [23], [24], [25]. The observed vertical increase in Ni grade in this study is therefore consistent with modern models of lateritic profile evolution, which highlight the preferential accumulation of nickel in saprolite relative to the overlying limonite zone under intense tropical weathering regimes.

3.3. Mechanism of Nickel Enrichment

Nickel enrichment within the saprolite zone is controlled by complex lateritic weathering processes and the evolving geochemical stability of host minerals. During intense tropical weathering of

ultramafic rocks, mobile elements such as magnesium and silica are progressively leached from the upper profile, while relatively immobile iron is retained and precipitated as secondary Fe-oxyhydroxides, primarily goethite and hematite, within the limonite zone [22]. These Fe phases exhibit high surface reactivity and are known to incorporate Ni through adsorption, surface complexation, and limited structural substitution within goethite lattices [26].

With increasing depth and progressive weathering evolution, variations in pH, redox (Eh) conditions, and groundwater percolation alter the stability and reactivity of Fe-oxyhydroxides, thereby affecting their capacity to retain Ni [27]. Under these evolving conditions, nickel may be progressively released from Fe phases and transported downward through percolating fluids. In the saprolite zone, Ni becomes preferentially enriched within Mg-rich silicate minerals such as serpentine, olivine-derived phases, and secondary Ni-bearing silicates, where it is incorporated through solid-solution substitution and secondary mineral precipitation processes [9], [26].

This coupled adsorption–desorption and dissolution–reprecipitation system explains the vertical partitioning of Ni in lateritic profiles, where the limonite zone acts as a transient Ni reservoir controlled by Fe-oxyhydroxides, while the saprolite zone represents the principal environment for long-term Ni accumulation under evolving physicochemical conditions characteristic of tropical weathering systems [22].

3.4. Multi-Element Interaction and Geochemical Interpretation

In addition to Fe and Ni, other elements such as MgO, SiO_2, and Al_2O_3 also significantly influence the geochemical characteristics and mineralogical classification of lateritic deposits [28]. The increase of MgO and SiO_2 concentrations in deeper layers indicates the dominance of magnesium-rich silicate minerals, such as serpentine and garnierite, within the saprolite zone [29].

The presence of Al_2O_3 is typically more pronounced in the upper limonite or bauxite-rich layers, reflecting the residual concentration of relatively immobile aluminum during the advanced stages of chemical weathering [30]. Monitoring the ratios of these components, such as the SiO_2/MgO ratio, is essential for determining the degree of serpentinization and the potential for nickel silicate enrichment within the weathering profile [29].

Based on the geochemical analysis results using the Energy Dispersive X-Ray Fluorescence (ED-XRF) method, the distribution of nickel (Ni) within the laterite profile is significantly influenced by the concentration of metal oxides and other silicate minerals. The following is a detailed description of the role of each chemical component in determining the characteristics of the limonite and saprolite zones and their relationship to nickel enrichment:

3.4.1. Fe_2O_3 (Iron Oxide)

The Fe_2O_3 content shows a pronounced vertical distribution pattern across the lateritic profile, with significantly higher concentrations in the limonite zone (71.40%-69.97%), reflecting the dominance of iron oxide minerals such as goethite and hematite under strongly oxidizing conditions. In contrast, a sharp decline in Fe_2O_3 is observed upon transition into the saprolite zone, where values decrease substantially to 30.05% at 6 m depth [31]. This trend indicates the preferential stability and accumulation of Fe in the upper oxidation zone during intense tropical weathering. Conversely, nickel (Ni) exhibits a clear inverse relationship with Fe_2O_3, increasing from 0.70% in the upper limonite zone to 2.05% in the deeper saprolite zone. This negative correlation supports the geochemical behavior typical of lateritic systems, where Fe is retained in the form of stable iron oxides in the limonite zone, while Ni is progressively mobilized through leaching processes and subsequently enriched in the

saprolite zone via incorporation into secondary silicate minerals and precipitation under changing physicochemical conditions.

3.4.2. MgO (Magnesium Oxide)

In the limonite zone, MgO content is relatively low, ranging from 1.49% to 1.73%, indicating extensive leaching of magnesium during advanced weathering stages. In contrast, a significant increase in MgO is observed in the saprolite zone, reaching up to 13.19%, reflecting the preservation and re-enrichment of Mg-bearing silicate minerals. This vertical trend shows a strong positive association between MgO and Ni distribution, where both elements increase with depth. The simultaneous enrichment of MgO and Ni highlights the important role of primary ultramafic minerals such as serpentine and olivine, which act as major Mg-rich phases and also serve as structural hosts for nickel through substitution within their crystal lattices or incorporation into secondary silicate minerals such as garnierite [9], [32]. Furthermore, elevated MgO content serves as an indicator of relatively less weathered ultramafic protoliths, where nickel remains associated with Mg-silicate phases in the saprolite zone rather than being fully liberated and redistributed, thereby reinforcing the role of silicate-hosted Ni mineralization in deeper lateritic profiles [33].

3.4.3. SiO_2 (Silica)

The SiO_2 content reflects the abundance of silicate minerals within the lateritic profile, with relatively low values in the limonite zone (5.78–6.98%) and a marked increase in the saprolite zone, reaching 29.16%. This sharp rise indicates the dominance of silicate minerals such as serpentine, talc, and olivine in the saprolite, which are recognized as the primary host phases for nickel in lateritic systems [34]. The concurrent increase of both SiO_2 and Ni with depth further reinforces the strong association between nickel enrichment and silicate mineralization processes, where Ni is structurally incorporated into Mg-rich silicate phases or secondary minerals formed during advanced weathering.

3.4.4. Al_2O_3 (Aluminum Oxide)

The Al_2O_3 content is relatively high in the limonite zone (7.85–9.06%), reflecting the presence of secondary aluminum-bearing minerals such as gibbsite, boehmite, and kaolinite formed under intense weathering conditions. In contrast, Al_2O_3 decreases significantly in the saprolite zone, ranging from 5.41% to 1.68%, indicating a progressive loss of clay minerals with depth. This downward trend suggests a clear mineralogical transition from Al-rich clay phases in the limonite zone to Mg-silicate–dominated assemblages in the saprolite zone. The decrease in Al_2O_3 coincides with increasing Ni enrichment, supporting the shift from aluminum-bearing weathering products to nickel-hosting Mg-silicate minerals during lateritic profile evolution [33].

3.4.5. Co (Cobalt)

High in limonite (0.12 to 0.06) and relatively constant in saprolite (0.09 to 0.05). Cobalt generally correlates with Fe, thus it tends to decrease as Ni increases.

3.4.6. MnO (Manganese Oxide)

Higher in limonite (1.04%) compared to saprolite (0.46%). This also strengthens the characterization of limonite as a layer rich in oxide metals other than nickel.

3.4.7. Cr_2O_3 (Chromium Oxide)

Cr_2O_3 is generally formed from chromite minerals that are resistant to weathering and commonly found in ultramafic rocks. The Cr_2O_3 content is relatively stable and increases slightly from 1.93% (1 m)

to 2.08% (3 m) within the limonite zone. However, Cr_2O_3 decreases upon entering the saprolite zone from 1.80% to only 1.18% at a depth of 6 meters, even though Ni continues to rise.

3.4.8. CaO (Calcium Oxide)

CaO shows very low content throughout the laterite profile, ranging from 0.02% in the limonite zone to a maximum of 0.39% in the saprolite zone. Although it increases slightly in the saprolite, the distribution of CaO shows no significant correlation with Ni content, which continues to increase from limonite to saprolite. This indicates that Ca does not play a role in the formation or enrichment of nickel and is likely present only in trace amounts from secondary minerals or minor carbonates.

The positive relationship between Ni and MgO/SiO2 suggests that nickel is associated with silicate mineral structures rather than iron oxide phases [31], [35]. Meanwhile, Al_2O_3 concentration tends to decrease with increasing depth, indicating a transition from clay-rich limonite layers toward silicate-rich saprolite layers [31].

3.5 Practical and Environmental Implications

The findings of this study provide important implications for nickel exploration and mining management [1], [18], [33]. The identification of saprolite as the primary nickel enrichment zone, characterized by a significant decrease in Fe content, can improve exploration efficiency and assist mining companies in identifying economically valuable ore zones more accurately [1], [23]. After nickel mining, which significantly reduces the content of iron and other nutrients in the soil, post-mining land generally undergoes severe physical, chemical, and biological degradation [35]. The soil becomes compacted, depleted of organic matter, and often loses the structure and porosity necessary to support plant growth. Therefore, reclamation efforts must be comprehensive, starting with the initial stage of returning the topsoil layer [24]. This layer is rich in organic matter, microorganisms, and both macro and micronutrients that are vital for restoring soil productivity.

However, in many cases, topsoil is lost or mixed with nutrient-poor subsoil during mining activities. In such conditions, the addition of soil ameliorants such as compost, manure, or biochar becomes a crucial step to improve soil aggregation and aeration [36]. These materials increase the soil's capacity to retain water and nutrients, providing a supportive environment for soil microbial activities that play a role in nutrient cycling.

Although iron content in post-mining soils may decline, it remains an essential micronutrient for plant physiological processes such as photosynthesis and enzymatic activity, and its availability can be enhanced through organic matter decomposition or the application of micronutrient-enriched fertilizers [37]. Effective reclamation also relies on biological approaches, particularly the use of pioneer species such as *Acacia mangium* and selected legumes, which are capable of tolerating nutrient-poor conditions while improving soil structure and accelerating topsoil formation. Over time, the sustainability of post-mining land restoration depends on the balanced interaction between soil, water, and vegetation, supported by continuous monitoring of soil physical and chemical properties to ensure ecosystem recovery [21], [34]. From an environmental standpoint, intensive laterite mining may alter soil mineral composition, including reductions in Fe and Mg content, highlighting the importance of sustainable mining and effective reclamation practices to mitigate degradation. In this context, ED-XRF analysis provides a rapid and non-destructive method for multi-element characterization, supporting efficient monitoring and decision-making in post-mining environmental management and nickel resource utilization [38].

4. Conclusion

The study results demonstrate that variations in iron (Fe) content significantly influence the distribution of nickel (Ni) within the laterite profile. In the limonite zone, high Fe concentrations ranging from 50.23-48.76% are associated with relatively low Ni contents of 0.70-1.15%. In contrast, within the saprolite zone, a decrease in Fe content to 29.41-21.01% is accompanied by a substantial increase in Ni levels to 1.45-2.05%. This trend indicates an inverse relationship between Fe and Ni, where the iron oxide-rich limonite zone is generally depleted in nickel, while the silicate-rich saprolite zone serves as the primary site of nickel enrichment. Furthermore, ED-XRF analysis successfully identified the quantitative distribution patterns of Fe and Ni across the different laterite zones. The Fe data obtained through ED-XRF are consistent with typical lateritic geochemical trends, showing that the decline in Fe content from the upper limonite layer to the lower saprolite layer corresponds to an increase in Ni concentration. Therefore, ED-XRF has proven to be an effective method for mapping elemental distribution and supporting the evaluation of the economic potential of nickel-bearing zones within laterite profiles.

Author contributions: Conceptualization, J.W.A.; methodology, J.W.A.; investigation, J.W.A.; data curation, J.W.A. and I. A; formal analysis, J.W.A.; writing—original draft preparation, I. A; writing—review and editing, J.W.A. The author has read and agreed to the published version of the manuscript.

Acknowledgement: The author would like to thank PT. Genba Multi Mineral, North Morowali for providing the nickel laterite samples used in this research. This research received no specific grant from any funding agency in the public, commercial, or not-for-profit sectors..

Conflict of Interest: The author declares no conflicts of interest..

5. References

[1] S. Stanković, S. Stopić, M. Sokić, B. Marković, and B. Friedrich, "Review of the past, present, and future of the hydrometallurgical production of nickel and cobalt from lateritic ores," *Metall Mater Eng*, vol. 26, no. 2, pp. 199–208, Jul. 2020, https://doi.org/10.30544/513

[2] L. Soh Tamehe, Y. Zhao, W. Xu, and J. Gao, "Ni(Co) Laterite Deposits of Southeast Asia: A Review and Perspective," *Minerals*, vol. 14, no. 2, p. 134, Jan. 2024, https://doi.org/10.3390/min14020134

[3] D. Deniyatno, M. Masri, R. I. M. C. Jaya, W. Wahab, and S. Syahrul, "Assessing the environmental impact of Kolaka peridotites from nickel mining waste for geological carbon storage: Mineralogy, carbonation potential, and rock property changes," *J. Degrade. Min. Land Manage.*, vol. 12, no. 5, pp. 8899–8911, Oct. 2025, https://doi.org/10.15243/jdmlm.2025.125.8899

[4] R. S. Harmon and G. S. Senesi, "GGR Handbook of Rock and Mineral Analysis Chapter 13 Laser-Induced Breakdown Spectroscopy (LIBS)," *Geostandard Geoanalytic Res*, vol. 48, no. 4, pp. 763–792, Dec. 2024, https://doi.org/10.1111/ggr.12560

[5] A. Ito, T. Otake, A. Maulana, K. Sanematsu, Sufriadin, and T. Sato, "Geochemical constraints on the mobilization of Ni and critical metals in laterite deposits, Sulawesi, Indonesia: A mass-balance approach," *Resource Geology*, vol. 71, no. 3, pp. 255–282, Jul. 2021, https://doi.org/10.1111/rge.12266

[6] Y. Choi, I. Lee, and I. Moon, "Geochemical and Mineralogical Characteristics of Garnierite From the Morowali Ni-Laterite Deposit in Sulawesi, Indonesia," *Front. Earth Sci.*, vol. 9, p. 761748, Nov. 2021, https://doi.org/10.3389/feart.2021.761748

[7] X. Wang *et al.*, "Efficient Utilization of Limonite Nickel Laterite to Prepare Ferronickel by the Selective Reduction Smelting Process," *Sustainability*, vol. 15, no. 9, p. 7147, Apr. 2023, https://doi.org/10.3390/su15097147

[8] S. Roy, H. Moustafa, K. Vaidya, J.-P. Harvey, and L. Fradette, "On process-based granular reconstruction of life cycle inventories: sustainably coherent planning of primary battery-grade nickel," Dec. 19, 2024, *In Review*. https://doi.org/10.21203/rs.3.rs-5639090/v1

[9] F. Putzolu *et al.*, "The Influence of the Magmatic to Postmagmatic Evolution of the Parent Rock on the Co Deportment in Lateritic Systems: The Example of the Santa Fé Ni-Co Deposit (Brazil)," *Economic Geology*, vol. 116, no. 4, pp. 837–861, Jun. 2021, https://doi.org/10.5382/econgeo.4819

[10] K. A. Aquino, C. A. Arcilla, C. Schardt, and C. A. J. Tupaz, "Mineralogical and Geochemical Characterization of the Sta. Cruz Nickel Laterite Deposit, Zambales, Philippines," *Minerals*, vol. 12, no. 3, p. 305, Feb. 2022, https://doi.org/10.3390/min12030305

[11] E. Mervine, R. Valenta, J. Paterson, G. Mudd, T. Werner, and L. Sonter, "Biomass carbon emissions from nickel mining have significant implications for climate action," Feb. 01, 2023, *In Review*. https://doi.org/10.21203/rs.3.rs-2469411/v1

[12] Z. R. Tshentu and D. Parajuli, "Editorial for the Special Issue on 'Recovery of Precious Metals, Rare Earth Elements and Special Metals from Spent Secondary Products,'" *Minerals*, vol. 12, no. 4, p. 481, Apr. 2022, https://doi.org/10.3390/min12040481

[13] K. A. Aquino, C. A. Arcilla, C. Schardt, and C. A. J. Tupaz, "Mineralogical and Geochemical Characterization of the Sta. Cruz Nickel Laterite Deposit, Zambales, Philippines," *Minerals*, vol. 12, no. 3, p. 305, Feb. 2022, https://doi.org/10.3390/min12030305

[14] C. V. Sagapoa, A. Imai, T. Ogata, and K. Yonezu, "Laterization Process Of Peridotites In Siruka, Choiseul, Solomon Islands". Vol. 3(2), pp. 76-92, Jul–Dec 2011.

[15] S. Wibowo, M. F. Rosana, and A. D. Haryanto, "Local Topographic Model using Position Index for Analyzing the Characteristics of Unserpentinized Lateritic Zones in Sorowako Nickeliferous Laterite Deposit, Indonesia," *International Journal on Advanced Science, Engineering and Information Technology*, vol. 8, no. 4, p. 1138, Aug. 2018, https://doi.org/10.18517/ijaseit.8.4.3509

[16] M. Mustafa, A. Maulana, U. R. Irfan, and A. Tonggiroh, "Determination of heavy metal elements concentration in soils and tailing sediments from lateritic nickel post-mining areas in Motui District, Southeast Sulawesi," *J.Degrade.Min.Land Manage.*, vol. 9, no. 2, pp. 3273–3279, Jan. 2022, https://doi.org/10.15243/jdmlm.2022.092.3273

[17] A. P. Faried, A. Tonggiroh, and U. R. Irfan, "Geochemical Characterization Of Bedrock And Distribution Of Enrichment Of Rare Earth Elements And Scandium In Nickel Laterite Within The Wulu Area, Central Buton District, Southeast Sulawesi Province," *IOP Conf. Ser.: Earth Environ. Sci.*, vol. 1451, no. 1, p. 012020, Feb. 2025, https://doi.org/10.1088/1755-1315/1451/1/012020

[18] P. Maurizot, B. Sevin, M. Iseppi, and T. Giband, "Nickel-Bearing Laterite Deposits in Accretionary Context and the Case of New Caledonia: From the Large-Scale Structure of Earth to Our Everyday Appliances," *GSAT*, vol. 29, no. 5, pp. 4–10, May 2019, https://doi.org/10.1130/GSATG364A.1

[19] C. Domènech and C. Villanova-de-Benavent, Eds., *Geochemistry and Mineralogy of Ni-Co Laterite Deposits*. MDPI, 2023. https://doi.org/10.3390/books978-3-0365-9630-3

[20] S. Stanković, S. Stopić, M. Sokić, B. Marković, and B. Friedrich, "Review of the past, present, and future of the hydrometallurgical production of nickel and cobalt from lateritic ores," *Metall Mater Eng*, vol. 26, no. 2, pp. 199–208, Jul. 2020, https://doi.org/10.30544/513

[21] V. Miettinen, J. Mäkinen, E. Kolehmainen, T. Kravtsov, and L. Rintala, "Iron Control in Atmospheric Acid Laterite Leaching," *Minerals*, vol. 9, no. 7, p. 404, Jun. 2019, https://doi.org/10.3390/min9070404

[22] S. Stanković *et al.*, "Options for Hydrometallurgical Treatment of Ni-Co Lateritic Ores for Sustainable Supply of Nickel and Cobalt for European Battery Industry from South-Eastern Europe and Turkey," *Metals*, vol. 12, no. 5, p. 807, May 2022, https://doi.org/10.3390/met12050807

[23] M. Osali *et al.*, "Selective Extraction of Nickel and Cobalt from Limonitic Laterite via Optimized Sulfation Roasting–Water Leaching and Solvent Extraction," *Minerals*, vol. 16, no. 5, p. 431, Apr. 2026, https://doi.org/10.3390/min16050431

[24] W. Wang *et al.*, "Preparation of Nickel–Iron Concentrate from Low-Grade Laterite Nickel Ore by Solid-State Metalized Reduction and Magnetic Separation," *Minerals*, vol. 14, no. 9, p. 926, Sep. 2024, https://doi.org/10.3390/min14090926

[25] U. König, "Nickel Laterites—Mineralogical Monitoring for Grade Definition and Process Optimization," *Minerals*, vol. 11, no. 11, p. 1178, Oct. 2021, https://doi.org/10.3390/min11111178

[26] C. Innocent, W. Kloppmann, R. Millot, and L. Vaute, "A multi-isotopic study of the groundwaters from the Lower Triassic Sandstones aquifer of northeastern France: Groundwater origin, mixing and flowing velocity," *Applied Geochemistry*, vol. 131, p. 105012, Aug. 2021, https://doi.org/10.1016/j.apgeochem.2021.105012

[27] B. Hu, Q. Zhang, S. Li, H. Yu, X. Wang, and H. Wang, "Application of Numerical Simulation Methods in Solving Complex Mining Engineering Problems in Dingxi Mine, China," *Minerals*, vol. 12, no. 2, p. 123, Jan. 2022, https://doi.org/10.3390/min12020123

[28] F. Wang and D. Dreisinger, "Acceleration of Iron-Rich Olivine CO2 Mineral Carbonation and Utilization for Simultaneous Critical Nickel and Cobalt Recovery," *Minerals*, vol. 14, no. 8, p. 766, Jul. 2024, https://doi.org/10.3390/min14080766

[29] T. Cheng, W. Yang, C. Teng, X. Yang, and D. Xiao, "Geochronology and Geochemistry of the Uhelchulu Quartz Diorite-Granodiorite in Inner Mongolia of China: Implications for Evolution of the Hegenshan Ocean in the Early-Middle Devonian," *Minerals*, vol. 14, no. 8, p. 835, Aug. 2024, https://doi.org/10.3390/min14080835

[30] Y. Teitler, S. Favier, J.-P. Ambrosi, B. Sevin, F. Golfier, and M. Cathelineau, "Evaluation of Sc Concentrations in Ni-Co Laterites Using Al as a Geochemical Proxy," *Minerals*, vol. 12, no. 5, p. 615, May 2022, https://doi.org/10.3390/min12050615

[31] D. Yessengaliyev *et al.*, "Application of a complex Si–Al–Fe reducing agent for the production of a nickel-containing alloy," *Sci Rep*, vol. 16, no. 1, p. 14856, Mar. 2026, https://doi.org/10.1038/s41598-026-45605-y

[32] O. V. Dickson, T. Deleau, F. Espitalier, C. Coquelet, J. Lombart, and V. Nallet, "Autoclave scaling behaviour and characterisation during nickel laterite ore leaching under HPAL conditions," *Cleaner Waste Systems*, vol. 14, p. 100503, Jun. 2026, https://doi.org/10.1016/j.clwas.2026.100503

[33] R. Schodde, "Nickel: A tale of two cities," 2025. https://doi.org/10.1016/j.geogeo.2025.100356

[34] B. Suleimen *et al.*, "Comparative Review of Processing Technologies for Oxidized (Lateritic) Nickel Ores," *Applied Sciences*, vol. 16, no. 9, p. 4478, May 2026, https://doi.org/10.3390/app16094478

[35] A. Eljoudiani *et al.*, "Technological Characterization of Cobalt and Nickel Ores from Greece for Metal Recovery". *Separations*, 11, 345, 2024, https://doi.org/10.3390/separations11120345

[36] H. Hasria *et al.*, "Mineralogy and Geochemical Characteristics of Lateritic Nickel Deposit in Wiwirano District, North Konawe, SE Sulawesi, Indonesia," *IGJ*, pp. 171–183, Sep. 2024, https://doi.org/10.46717/igj.57.2C.13ms-2024-9-21

[37] R. Eso *et al.*, "Using Soil Magnetic Susceptibility Proxies to Estimate Overburden Thickness Overlying Ore of Lateritic Soils in Sulawesi Island Indonesia," *IGJ*, pp. 17–32, Jun. 2024, https://doi.org/10.46717/igj.57.1F.2ms-2024-6-11

[38] D.-R. Qi, T.-G. Lan, Q. Shu, Y. Feng, and S.-H. Zhou, "Nickel enrichment during lateritization of ophiolitic ultramafic rocks: A case study from the Kelurahan Pondidrha laterite profile in Sulawesi, Indonesia," *Ore Geology Reviews*, vol. 170, p. 106140, Jul. 2024, https://doi.org/10.1016/j.oregeorev.2024.106140